

NMR Study of the Magnetic and Metal-Insulator Transitions in $\text{Na}_{0.5}\text{CoO}_2$: A Nesting Scenario

J. Bobroff,¹ G. Lang,¹ H. Alloul,¹ N. Blanchard,¹ and G. Collin²

¹Laboratoire de Physique des Solides, UMR8502, Université Paris XI, 91405 Orsay, France

²LLB, CE-Saclay, CEA-CNRS, 91191 Gif Sur Yvette, France

(Received 22 July 2005; published 13 March 2006)

Co and Na NMR are used to probe the local susceptibility and charge state of the two Co sites of the Na-ordered orthorhombic $\text{Na}_{0.5}\text{CoO}_2$. Above $T_N = 86$ K, both sites display a similar T dependence of the spin shift, suggesting that there is no charge segregation into Co^{3+} and Co^{4+} sites. Below T_N , the magnetic long range commensurate order found is only slightly affected by the metal-insulator transition at $T_{\text{MIT}} = 51$ K. Furthermore, the electric field gradient at the Co site does not change at these transitions, indicating the absence of charge ordering. All these observations can be explained by successive spin-density wave induced by two nestings of the Fermi surface specific to the $x = 0.5$ Na ordering.

DOI: 10.1103/PhysRevLett.96.107201

PACS numbers: 75.30.Fv, 71.27.+a, 71.30.+h, 76.60.-k

The Na_xCoO_2 cobaltates consist of two-dimensional Co triangular layers of which doping can be varied by changing the Na content. Even though doped layers of transition ions seem similar to the CuO_2 planes of high- T_C cuprates, their physical properties are strikingly different. The Na_1CoO_2 composition is a band insulator made of filled-shell nonmagnetic Co^{3+} [1]. At $x < 1$, the system becomes metallic, but only specific Na compositions can be obtained, which correspond to some Na orderings as observed by crystallography. Such Na orderings may turn into charge orderings among Co planes as the Co valence state depends on the Co position relative to the Na ion [2,3]. For $x > 0.6$, strong electronic correlations are observed between Co, revealed by a Curie-Weiss $1/(T + \Theta)$ susceptibility with $\Theta \sim 100$ K. At lower Na content, i.e., higher doping, the compound becomes more metallic as evidenced by a Pauli-like susceptibility and an increase of the Drude weight in optics, except for $x = 0.5$ [4]. At $x = 0.3$, the system can even be superconducting when water molecules are intercalated between Na and CoO_2 layers [5]. However, this apparent smooth evolution in the phase diagram from a correlated to a noncorrelated metal shows a sharp discontinuity at $x = 0.5$. At this composition, Na orders in an orthorhombic superstructure commensurate with the Co lattice. $\text{Na}_{0.5}\text{CoO}_2$ is a poor metal, with resistivity about 20 times larger than at other Na contents, and shows a metal-insulator transition at $T_{\text{MIT}} = 51$ K [2]. In addition, it displays a long range magnetic order below $T_N = 86$ K, a Néel temperature much higher than those measured at higher doping contents [2,6]. At the same T_N , the Hall coefficient and thermoelectric power change sign, while a small kink is observed on resistivity [2]. Such peculiarities have been interpreted in terms of a charge ordering (CO) in the Co layers induced by the Na orthorhombic order [2,4,7]. Assuming the Co ion is a filled-shell $3+$ state when it locates at the vertical of a Na ion, and a $4 + S = 1/2$ state otherwise, the Na superstructure should result in a charge segregation between rows of nonmagnetic Co^{3+} and magnetic Co^{4+} , leading to the observed insulating magnetic behavior. However, this interpretation

fails to explain why CO takes place only at T_{MIT} , while Na order is already observed at room temperature. It is also hard to reconcile with the fact that magnetic order takes place at $T_N \neq T_{\text{MIT}}$.

In order to state the actual existence of CO, we have performed a ^{59}Co and ^{23}Na NMR study which allows us to differentiate the two Co sites and to give indications on their valence state through their paramagnetic and quadrupolar parameters. Our results allow us to establish that the simple ionic charge segregation picture into Co^{3+} - Co^{4+} does not occur either at T_N or at T_{MIT} . Instead, we propose an interpretation in terms of a metallic band in which two successive spin-density wave transitions are driven by two nestings of the Fermi surface. This scenario reconciles transport and magnetic measurements.

NMR measurements were carried out on orthorhombic $\text{Na}_{0.5}\text{CoO}_2$ obtained similarly to that of Ref. [6]. Crystallites were aligned along their c axis in epoxy in a 7 T applied field. NMR spectra were obtained by either sweeping the field or the frequency and reconstructing the spectrum through Fourier transform recombinations. The nuclear resonance is a probe of the local spin susceptibility through the shift $K_c = A_{\text{hf}}^c \chi / \mu_B + K_c^{\text{orb}}$ where χ is the electronic susceptibility, A_{hf}^c is the hyperfine coupling, and K_c^{orb} is an orbital T -independent term. It is also sensitive to the surrounding charges through the electric field gradient (EFG) proportional to the quadrupolar frequencies $\nu_Q^{j=a,b,c} \propto Q \partial^2 V / \partial j^2$ where Q is the quadrupolar moment. For a nuclear spin I , these parameters are measured through the detection of the different resonant frequencies for each transition $m \leftrightarrow m - 1$ ($m = I, I - 1, \dots, -I + 1$), following:

$$\begin{aligned} \nu_{m \leftrightarrow m-1}^c &= \nu_0(1 + K_c) + (0.5 - m)\nu_Q^c \\ &+ a(\nu_Q^a - \nu_Q^b)^2 / \nu_0, \end{aligned}$$

where the field H_0 is applied along the c axis, with $\nu_0 = \gamma / 2\pi H_0$, γ is the gyromagnetic ratio, and a depends on m and I .

Since the orbital shift is almost negligible in the case of ^{23}Na NMR, the Na shift is directly proportional to the average Co layer spin susceptibility through hyperfine couplings between Na and Co [3]. Figure 1 displays this shift as determined from the frequency of the $-1/2 \leftrightarrow 1/2$ transition corrected from second order quadrupolar effects. For $T > 210$ K, the line shape is narrow and no quadrupolar satellite is detected. This results from the occurrence of Na ionic diffusion, as also revealed by a sharp minimum in transverse relaxation time T_2 observed as well in $\text{Na}_{0.7}\text{CoO}_2$ [8]. At $T < 210$ K, the motion of the Na ions freezes, and the two Na crystallographic sites can be resolved, but are found to display similar shifts. We shall go back to the low T magnetic regime later. The macroscopic susceptibility χ_m is plotted on Fig. 1 as well, using a hyperfine coupling scaling factor close to that of $\text{Na}_{0.7}\text{CoO}_2$. The Na shift shows the same T dependence as χ_m as expected. This allows us to extract the orbital contribution $\chi_{\text{orb}} = 2.1 \times 10^{-4}$ emu/mol, which amounts to about 50% of the macroscopic susceptibility at room T . The spin susceptibility decreases with temperature, by about 25% between $T = 300$ K and T_N . This deviation to a pure Pauli-constant behavior could be due to the strong correlations present in the 2D Co layer or any T dependence of the Fermi level density of states.

Co NMR can then be used to measure independently the contribution of the two crystallographic Co sites to this susceptibility. We, indeed, identified two sets of Co NMR signals, called A and B hereafter, with similar weights corresponding to the two Co sites of the unit cell. Their quadrupolar frequencies $\nu_Q^c = 2.8$ and 4 MHz agree with the findings of Ref. [9]. Site A falls into two subsets A_1 and A_2 with slightly different ν_Q^c and the same intensities [10]. The different Co shifts K_C are deduced from the measurement of the different quadrupolar transitions at each temperature. Their T dependence, plotted on Fig. 2, mimics that of χ_m like Na shifts do. The scaling between K_C and χ_m leads to $A_{\text{hf}}^c = 18 \pm 3$ T for both A and B sites, and $K_c^{\text{orb}} = 1.32\%$, 1.36% , $1.57\% \pm 0.2\%$ for A_1 , A_2 , and B .

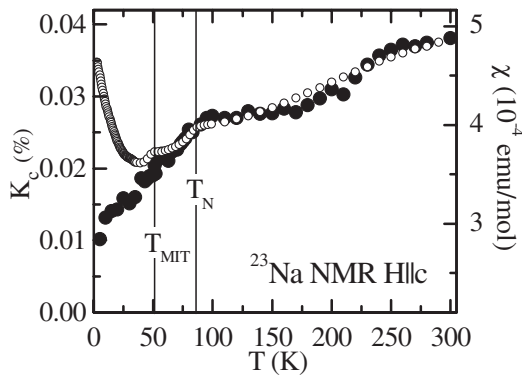


FIG. 1. Na NMR spin shift K_C of both Na sites (left axis, full circles) compared to the macroscopic susceptibility in nonoriented powder (right axis, empty circles, $H = 0.1$ T).

The fact that both A and B shifts behave similarly with the same hyperfine coupling demonstrates that neither one can be Co^{3+} above T_N . If the Co charge was $3+$, one would expect no T dependent spin shift at all and $K_c^{\text{orb}} = 1.9\%$ [1]. Furthermore, the hyperfine coupling A_{hf}^c lies between the values found in $\text{Na}_{0.7}\text{CoO}_2$ for $\text{Co}^{3.3+}$ ($A_{\text{hf}}^c = 4.2$ T) and $\text{Co}^{3.7+}$ ($A_{\text{hf}}^c = 24$ T), suggesting that the charge of both A and B lies between $3.5 \pm \varepsilon$ with $\varepsilon < 0.2$ [3]. Similar T dependences for shift and hyperfine couplings were found for $H_0 \perp c$ for site A , confirming our conclusions, while site B was too broad to be resolved in the perpendicular distribution pattern.

Let us now focus on the magnetically ordered regime below T_N . Frozen moments develop and induce magnetic splittings of the Co and Na NMR lines associated with the magnetic order. The A_1 Co line splits into two subsets shifted by $-h$ and $+h$ (the B Co signal is not detected anymore, possibly due to a shortening of its transverse relaxation time and/or a large broadening). Splittings with similar T dependence are observed as well for one Na site, as plotted on Fig. 3. At the other site, the transferred Co moments cancel with each other, so that it is not split. In addition to these splittings and contrary to the situation encountered in most antiferromagnets, a paramagnetic component in the magnetization can be detected here, which is found to be similar for both Na sites. This Na shift measured by the center of gravity of the spectra and plotted in Fig. 1 is not proportional to the macroscopic susceptibility anymore, neither to the frozen moment T dependence displayed in Fig. 3.

As Na is coupled to different Co sites from the two Co adjacent layers, the actual moment organization is hard to deduce. However, one can measure the effect of magnetic and metal-insulator transitions (MIT) on the charge of the Co site through its quadrupolar parameter and on the Co moments through their magnetic splittings. On the charge side, the quadrupolar parameter ν_Q^c of the Co A_1 site displayed in Fig. 3 stays constant below $T = 100$ K within

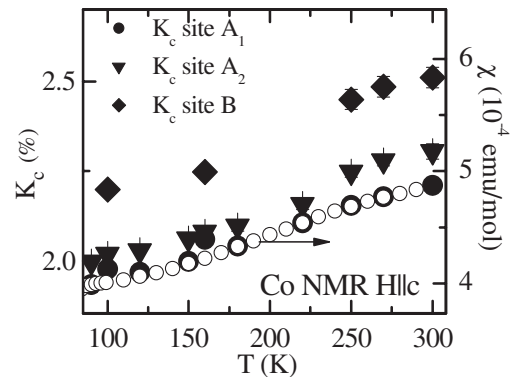


FIG. 2. Co NMR spin shifts K_C for the three Co sites (A_1 and A_2 correspond to one crystallographic site, and B to the other) (left axis, full symbols) compared to macroscopic susceptibility in nonoriented powder (empty circles, right axis).

an incertitude of 0.7%. On the contrary, any CO at T_N or T_{MIT} would result in a change of the EFG on this Co site. In an ionic point charge model, a CO modifying Co layers into alternated chains of Co^{3+} and Co^{4+} should change ν_Q^c by 19%. The constant behavior of ν_Q^c evidences the absence of any total CO below T_N while magnetic order develops. Anyhow, a small disproportionation into $\text{Co}^{3+\varepsilon}\text{-Co}^{4-\varepsilon}$ could exist, with $\varepsilon < 0.2$.

On the magnetic side, the ordering appears commensurate with the lattice. Otherwise, a continuous frequency distribution would be observed instead of the narrow α and β lines for Na NMR. Each Na ion is equally coupled to its two adjacent Co layers. One can thus rule out any simple antiferromagnetic order between planes, which would induce no splitting of all Na lines. The accurate measurement of the Na splitting α done on Fig. 3 shows a sharp magnetic transition at T_N , with a very small change at T_{MIT} .

All our results are inconsistent with a charge ordering or a Mott-like MIT scenario. Not only do T_{MIT} and T_N not coincide, but both results in the metallic and ordered states are incompatible with a simple CO with alternated rows of Co^{3+} and Co^{4+} . We propose to explain both the MIT and magnetic transitions by a new scenario, invoking two successive nestings of the Fermi surface (FS). When two portions of a FS can be nested with each other by a vector \vec{Q} , this may lead at low enough temperature to either a spin density wave (SDW) or charge density wave (CDW) with a modulation of charge or spin of frequency \vec{Q} [11]. Angle-resolved photoemission spectroscopy (ARPES) measurements for $x = 0.48$ reveal a FS with hexagonal shape, as shown in Fig. 4 [12]. At $x = 0.5$, the specific ordering of

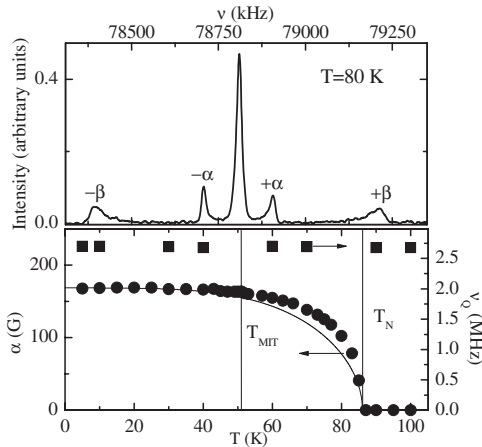


FIG. 3. Upper panel: Na NMR central transition below T_N where frozen moments induce $a \pm \alpha$ and $\pm\beta$ splitting of part of the central line. Lower panel, left axis: the T dependence of the splitting α , which is proportional to the c component of the local field resulting from frozen moments (circles) together with a BCS weak-coupling fit (line). Right axis: the quadrupolar frequency ν_Q^c of Co A site proportional to electric field gradient along the c axis.

Na ions transforms the unit cell from hexagonal to orthorhombic. This in turn changes the Brillouin zone (BZ) into a smaller rectangle which now cuts the FS as shown in Fig. 4. In the presence of any small lattice potential, gaps should open at the intersections between BZ and FS and lead to a curvature of the FS as plotted on Fig. 4. Three different nestings \vec{Q}_1 , \vec{Q}_2 , and \vec{Q}_3 , are now possible. As \vec{Q}_1 nests larger regions of the FS, it should occur at a higher temperature, i.e., $T_N = 86$ K. It would naturally lead to a SDW compatible with our present NMR results. As $\vec{Q}_1 \approx (2/3; 1/3)$ in hexagonal reciprocal cell units, it is commensurate with the Co lattice and must lead to a commensurate SDW, as observed here. The magnetic moment T dependence in Fig. 3 shows an increase near T_C slightly sharper than in the weak-coupling BCS limit, similar to other SDW systems [11]. The associated opening of a gap on the nested parts of the FS is observed in optics below $T \sim 100$ K [5] as well as in resistivity [4]. The carriers responsible for transport are now linked to the non-nested corners of the FS, which explains then the change of sign of the Hall coefficient at T_N . The next transition at $T_{MIT} = 51$ K originates from a second nesting between the residual pockets. This nesting is expected to occur at \vec{Q}_3 more likely than \vec{Q}_2 since it nests larger regions of FS. But ARPES measurements are needed to determine the exact nesting vector which will be very dependent on the actual shape of the pockets. This second nesting would leave very few carriers at the Fermi level, explaining the sharp “MIT” increase in resistivity and the observed large vanishing of the FS [13]. The presence of residual small pockets would then be due to the non-nested parts of FS, which could be partly responsible for the observed susceptibility measured by Na NMR below T_N . If this nesting leads to a SDW as well, the resulting magnetic order would then mix up both

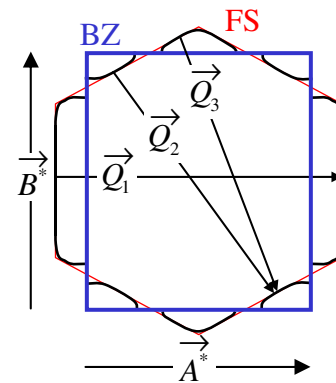


FIG. 4 (color online). Extended zone scheme of the reciprocal lattice. At $x = 0.5$, the Brillouin zone (BZ) is a rectangle (blue contour) due to the Na ordering, with reciprocal unit vectors A^* and B^* . This should transform the hexagonal Fermi surface FS measured in Ref. [12] at $x = 0.48$ (red contour) into the black contour. In this new FS, three possible nestings \vec{Q}_1 , \vec{Q}_2 , and \vec{Q}_3 are identified.

\vec{Q}_1 and \vec{Q}_3 modulations, likely with a much smaller weight associated with \vec{Q}_3 . Hence, only a small modification to the existing moments would be observed at T_{MIT} , in agreement with our findings, while magnetic ordering could be slightly affected, as observed by muon spin resonance [6]. The anomalies detected also at $T = 30$ K in both resistivity and magnetism [2,6] could be linked to a further instability here again linked to a nesting of the remaining pockets. Electron diffraction studies reveal the presence of an additional superstructure observed below $T = 100$ K [2]. This may stem from a coupling between the two successive SDWs and the lattice, similar to that observed in Cr or organic compounds [14]. The succession of two CDWs driven by two nestings has been observed in 1D or 2D metals such as NbSe₃ or monophosphate tungsten bronzes, together with a change in sign of the Hall coefficient very similar to the present case [15]. To our knowledge, Na_{0.5}CoO₂ is the first case where SDWs are involved.

In conclusion, our NMR results allow us to evidence that the Co³⁺-Co⁴⁺ charge order scenario does not apply in the Na-ordered Na_{0.5}CoO₂. We assign the magnetic transition to a SDW associated with a nesting of the FS. This explains both our NMR results and previous Hall, resistivity, and optical conductivity measurements. We attribute the MIT transition to a second nesting of the remaining FS pockets, which would explain the weak modifications of the magnetic order, while FS and resistivity are strongly affected. In our view, the $x = 0.5$ composition is peculiar in the phase diagram because the corresponding Na ordering favors specific nestings of the FS. In this scenario, the large Coulomb interaction U present in Co layers naturally provides the coupling necessary for the appearance of a SDW, and Na_{0.5}CoO₂ definitely belongs to the class of low dimensional strongly correlated materials. The magnetic orders observed for $x > 0.75$ with small magnetic moments could be explained in a SDW scenario as well. Here again, the associated Na orderings could trigger different nesting vectors and explain why T_N does not evolve monotonously with Na content. ARPES measurements are clearly needed to establish how the FS evolves with temperature and Na doping.

We acknowledge V. Brouet, N. Dupuis, P. Foury, M. Heritier, D. Jerome, P. Lederer, P. Mendels, I. Mukhamedshin, D. Nunez-Regueiro, J.P. Pouget, S. Ravy, and P. Wzietek for fruitful discussions.

Note added.—During completion of the manuscript, we became aware of a Co NMR and neutron study on the same

material focused mostly on the magnetic state, which corroborates our results [16]. However, in the proposed magnetic structure, no Na splitting should be observed contrary to our measurements. Another NMR study [17] submitted just after ours concludes that the ²³Na NMR data also support the absence of charge ordering at the magnetic transition. However, the sensitivity of the Na EFG to Co charge and the accuracy of their data are not sufficient to allow the authors to reach such conclusions independently of our results. An ARPES study submitted after ours reports the detection of a reconstruction of the Fermi surface due to Na ordering which appears consistent with our nesting scenario [18].

-
- [1] G. Lang *et al.*, Phys. Rev. B **72**, 094404 (2005).
 - [2] M.L. Foo *et al.*, Phys. Rev. Lett. **92**, 247001 (2004); Q. Huang *et al.*, J. Phys. Condens. Matter **16**, 5803 (2004); H.W. Zandbergen *et al.*, Phys. Rev. B **70**, 024101 (2004).
 - [3] I.R. Mukhamedshin, H. Alloul, N. Blanchard, and G. Collin, Phys. Rev. Lett. **93**, 167601 (2004); Phys. Rev. Lett. **94**, 247602 (2005).
 - [4] N.L. Wang *et al.*, Phys. Rev. Lett. **93**, 147403 (2004); J. Hwang, J. Yang, T. Timusk, and F.C. Chou, Phys. Rev. B **72**, 024549 (2005).
 - [5] K. Takada *et al.*, Nature (London) **422**, 53 (2003).
 - [6] P. Mendels *et al.*, Phys. Rev. Lett. **94**, 136403 (2005).
 - [7] K.W. Lee, J. Kunes, P. Novak, and W.E. Pickett, Phys. Rev. Lett. **94**, 026403 (2005); T.P. Choy, D. Galanakis, and P. Phillips, cond-mat/0502164.
 - [8] J.L. Gavilano *et al.*, Phys. Rev. B **69**, 100404 (2004).
 - [9] F.L. Ning, T. Imai, B. W. Statt, and F.C. Chou, Phys. Rev. Lett. **93**, 237201 (2004).
 - [10] J. Bobroff *et al.* (to be published).
 - [11] G. Grüner, Rev. Mod. Phys. **66**, 1 (1994).
 - [12] H.-B. Yang *et al.*, Phys. Rev. Lett. **95**, 146401 (2005); M.Z. Hasan *et al.*, cond-mat/0501530.
 - [13] L. Balicas *et al.*, Phys. Rev. Lett. **94**, 236402 (2005).
 - [14] J.P. Hill, G. Helgesen, and D. Gibbs, Phys. Rev. B **51**, 10336 (1995); J.P. Pouget and S. Ravy, J. Phys. I (France) **6**, 1501 (1996).
 - [15] N.P. Ong and P. Monceau, Phys. Rev. B **16**, 3443 (1977); R.M. Fleming, J.A. Polo, Jr., and R.V. Coleman, Phys. Rev. B **17**, 1634 (1978); C. Hess *et al.*, Phys. Rev. B **54**, 4581 (1996).
 - [16] M. Yokoi *et al.*, J. Phys. Soc. Jpn. **74**, 3046 (2005).
 - [17] B. Pedrini *et al.*, Phys. Rev. B **72**, 214407 (2005).
 - [18] D. Qian *et al.*, Phys. Rev. Lett. **96**, 046407 (2006).